# Thermodynamic and Steady-State Fluorescence Emission Studies on Metal Complexes of Receptors Containing Benzene Subunits

**M. Alexandra Bernardo,[†] Fernando Pina,*[,†] Enrique García-España,*[,‡] Julio Latorre,[‡] Santiago V. Luis,*[,||] José M. Llinares,[§] José A. Ramírez,[‡] and Conxa Soriano[§]**

Departamento de Química, Centro de Química Fina e Biotechnologia, Faculdade de Ciências e Tecnologia, Universidade Nova de Lisboa, Monte de Caparica, Portugal, Departament de Química Inorgànica, Facultat de Química, Universitat de València, C/ Dr. Moliner 50, 46100 Burjassot (València), Spain, Departament de Química Orgánica, Facultat de Farmacia, Universitat de València, Av. Vicente Andrés Estellés s/n, 46100 Burjassot (València), Spain, and Departamento de Química Inorgánica y Orgánica, Laboratorio de Química Orgánica, Universitat Jaume I, 12080 Castellón, Spain

*Received July 7, 1997*

The thermodynamic properties of the $Co^{2+}$, $Ni^{2+}$, $Cu^{2+}$, $Zn^{2+}$, $Cd^{2+}$, and $Pb^{2+}$ complexes of a family of N,N′-dibenzylated open-chain polyamines are described. For comparison, similar studies are reported for polyazacyclophane macrocyclic receptors containing an aromatic subunit linking the ends of a polyamine bridge. The metal complexes of the dibenzylated ligands show lower stability constants than those reported for related nonbenzylated open-chain polyamines. On the other hand, the stability constants of these complexes are clearly higher than those found for complexes of polyazacyclophane macrocycles containing a single para-substituted benzene spacer interrupting saturated polyamine bridges. All the studied complexes follow the Irving−Williams stability order. The crystal structure of $[Cu(\mathbf{L7})(H_2O)](ClO_4)_2$ (**L7** = 1-benzyl-1,5,8,12-tetrazadodecane) shows a very strongly axially distorted square planar coordination geometry for $Cu^{2+}$. Crystals of $[Cu(\mathbf{L7})(H_2O)](ClO_4)_2$ ($C_{15}H_{24}Cl_2CuN_4O_9$) are orthorhombic, space group $P2_12_12_1$, with $a = 7.586(1)$ Å, $b = 10.715(3)$ Å, and $c = 28.13(2)$ Å, $Z = 4$, $R_1 = 0.0572$, and $wR_2 = 0.1570$. Steady-state fluorescence emission studies performed on the $Cu^{2+}$ and $Zn^{2+}$ complexes show that, while none of the $Cu^{2+}$ complexes is emissive (CHEQ effect), fluorescence emission is observed for those $Zn^{2+}$ complexes with all the nitrogen donors either protonated or coordinated to the metal ions (CHEF effect). The composition of the frontier molecular orbitals of the free-ligands and of the $Cu^{2+}$ and $Zn^{2+}$ complexes supports this behavior. The use of these water-soluble ligands as chemosensors by means of enhancement or quenching of the fluorescence emission is also discussed.

## Introduction

Recently we have reported on the synthesis, protonation, and some aspects concerning the metal ion and anion coordination chemistry of a family of azacyclophane receptors containing a single aromatic ring between a saturated polyamine chain (see **L5** and **L6** in Chart 1).[1−6] The presence of the *p*-phenylene spacer induces interesting properties with respect to the protonation and metal ion coordination of these receptors. With regard to metal coordination, the spacer imposes enough stiffening in the polyamine chain to prevent the simultaneous coordination of both benzylic nitrogens to the same metal ion. Therefore, unsaturated and often low-symmetry coordination sites are obtained which are of interest in order to achieve particular reactivities such as stabilization of low-valent metal complexes or activation of hydrolytic pathways.[4,6] The low number of nitrogen atoms in the first coordination sphere of the metal complexes results in low stabilities for the mononuclear complexes in comparison with related open-chain or cyclic polyamines. However, since adequate open-chain counterparts of these receptors were not available, including both aromatic and polyamine moieties, we recently undertook the synthesis of a series of terminally dibenzylated open-chain polyamines (see Chart 1, compounds **L1**−**L4**). In a first report, we dealt with their synthetic procedure and with a potentiometric

[†] Universidade Nova de Lisboa.
[‡] Departament de Química Inorgànica, Universitat de València.
[§] Departament de Química Orgànica, Universitat de València.
[||] Universitat Jaume I.

(1) (a) Andrés, A.; Burguete, M. I.; García-España, E.; Luis, S. V.; Miravet, J. F.; Soriano, C. *J. Chem. Soc., Perkin Trans. 2* **1993**, 749. (b) Bianchi, A.; Escuder, B.; García-España, E.; Luis, S. V.; Marcelino, V.; Miravet, J. F.; Ramírez, J. A. *J. Chem. Soc., Perkin Trans. 2* **1994**, 1253.

(2) (a) Bencini, A.; Burguete, M. I.; García-España, E.; Luis, S. V.; Miravet, J. F.; Soriano, C. *J. Org. Chem*. **1993**, *58*, 4749. (b) Burguete, M. I.; Escuder, B.; García-España, E.; Luis, S. V.; Miravet, J. F. *J. Org. Chem*. **1994**, *59*, 1067. (c) Altava, B.; Burguete, M. I.; Escuder, B.; Luis, S. V.; García-España, E.; Muñoz, M. C. *Tetrahedron* **1997**, *53*, 2629.

(3) Andrés, A.; Bazzicalupi, A.; Bianchi, A.; García-España, E.; Luis, S. V.; Miravet, J. F.; Ramírez, J. A. *J. Chem.* Soc., *Dalton Trans.* **1994**, 2995.

(4) (a) Doménech, A.; Folgado, J. V.; García-España, E.; Luis, S. V.; Llinares, J. M.; Miravet, J. F.; Ramírez; J. A. *J. Chem. Dalton Trans.* **1995**, 541. (b) Doménech, A.; García-España, E.; Marcelino, V.; Altava, B.; Luis, S. V.; Miravet, J. F.; Bianchi, A.; Ferrini, L. *Inorg. Chim. Acta* **1996**, 123.

(5) (a) García-España, E.; Latorre, J.; Luis, S. V.; Miravet, J. F.; Pozuelo, P.; Ramírez, J. A.; Soriano, C. *Inorg. Chem.* **1996**, *35*, 4591. (b) García-España, E.; Latorre, J.; Marcelino, V.; Ramírez, J. A.; Luis, S. V.; Miravet, J. F.; Querol, M. *Inorg. Chim. Acta* **1997**, *256*, 179. (c) García-España, E.; Latorre, J.; Luis, S. V. *Supramol. Chem.* **1996**, *6*, 257.

(6) (a) Burguete, M. I.; Escuder, B.; Luis, S. V.; García-España, E.; Luis, S. V.; Miravet, J. F. *Tetrahedron Lett.* **1994**, 9075. (b) Altava, B.; Burguete, M. I.; Luis, S. V.; Miravet, J. F. García-España, E.; Marcelino, V.; Soriano, C. *Tetrahedron* **1997**, *53*, 4571.

S0020-1669(97)00840-9 CCC: $15.00 
Published on Web 07/07/1998

**Chart 1**

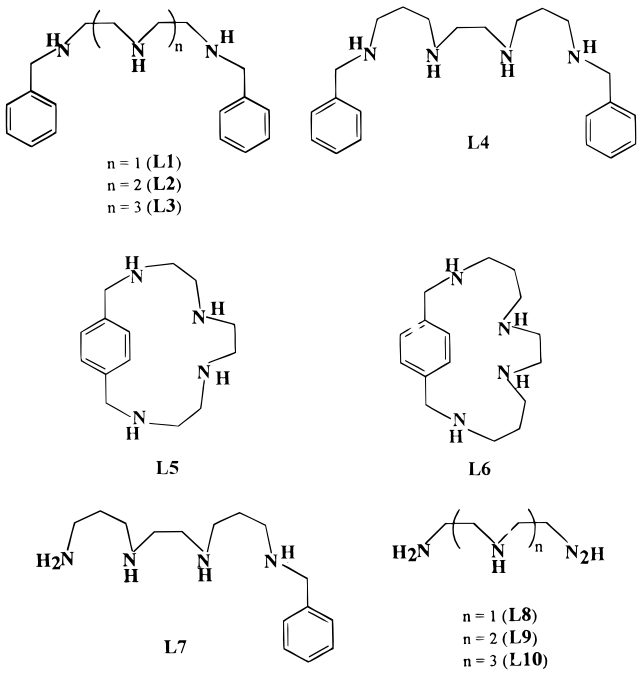


and photochemical study on their acid−base behavior as well as on aspects of their adduct formation with hexacyanocobaltate-(III).[7] The aromatic moieties present in these ligands cause them to exhibit fluorescence at room temperature,[7,8] thus steady-state fluorescence emission studies can be used to complement the potentiometric data. According to previous studies on the protonation of the polyazacyclophane macrocyclic receptors as well as on their analogous N,N′-dibenzylated open-chain polyamines,[7,8] the fully protonated forms display the largest emission intensities in both families. As the pH is increased, the consequent nitrogen deprotonation leads to a large decrease in the fluorescence emission intensity followed by minor changes in the shape of their respective spectra.

This quenching effect was attributed to the photoinduced electron transfer (PET) that can occur between the lone pair of the deprotonated amines in the polyamine chain, and the excited benzene moiety. Therefore, those receptors incorporating a polyamine chain and an aromatic subunit can be used as fluorescent chemosensors because their coordination to substrates, like protons, modifies the fluorescence emission of the benzene unit, signaling the receptor−substrate interaction.[9−19] Metal cations are another kind of substrate that can change the fluorescence pattern of the receptors. Coordination of these substrates can either enhance the fluorescence emission intensity (CHEF, chelation-enhanced fluorescence) or, alternatively, produce the opposite effect (CHEQ, chelation-enhanced quenching), whenever the substrate chelation leads to a decrease of the fluorescence emission intensity of the chemosensor.[9]

In this work we describe some CHEF and CHEQ effects, in aqueous solutions, resulting from chelation of metal ions by the above-mentioned families of fluorescent chemosensors.

## Experimental Section

**Materials.** Ligands **L1**−**L6** were synthesized as described previously[2,7] and handled as their hydroperchlorate salts. $NaClO_4$, used to keep the ionic strength constant, was purified according to ref 20. All the measurements were carried out in either 0.15 mol $dm^{-3}$ $NaClO_4$ or 0.15 mol $dm^{-3}$ NaCl. $CO_2$-free NaOH solutions and HCl or $HClO_4$ solutions were prepared following the procedure reported in ref 21.

**Synthesis of [Cu(L7)(H$_2$O)](ClO$_4$)$_2$.** In the preparative procedure of **L4** reported in ref 7, detosylation of (**L4**)$Ts_4$ yielded mainly dibenzylated **L4** and a small amount of **L7** as a result of the cleavage of one of the benzylic bonds. Addition of $Cu(ClO_4)_2 \cdot 4H_2O$ to an aqueous solution of the mixture, followed by evaporation at room temperature, afforded pink-blue crystals of the compound [Cu(**L7**)-$(H_2O)](ClO_4)_2$ suitable for X-ray diffraction analysis.

**CAUTION!** *Perchlorate salts of metal complexes of organic ligands are potentially explosive and should be handled with care.*

**Spectrophotometric and Spectrofluorimetric Titrations.** Absorption spectra were recorded on a Perkin-Elmer Lambda 6 spectrophotometer and fluorescence emission on a SPEX F111 Fluorolog spectrofluorimeter. $HClO_4$ and NaOH were used to adjust the pH values that were measured on a Metrohm 713 pH meter. All the measurements were carried out in either 0.15 mol $dm^{-3}$ $NaClO_4$ or 0.15 mol $dm^{-3}$ NaCl. Linearity of the fluorescence emission was checked in the concentration range used. The absorbance of the excitation wavelength was maintained lower than ca. 0.15. When excitation was carried out at wavelengths different from the isobestic points, a correction for the absorbed light was performed.

**Emf Measurements.** The potentiometric titrations were carried out in 0.15 mol $dm^{-3}$ $NaClO_4$ at 298.1 ± 0.1 K, except for **L4** for which NaCl 0.15 mol $dm^{-3}$ was used due to the low solubility of their complexes in the former medium. The experimental procedure (buret, potentiometer, cell, stirrer, microcomputer, etc.) has been fully described elsewhere.[22] The emf data were acquired with the computer program PASAT.[23] The reference electrode was an Ag/AgCl electrode in saturated KCl solution. The glass electrode was calibrated as an hydrogen-ion concentration probe by titration of previously standardized amounts of HCl with $CO_2$-free NaOH solutions and determining the equivalent point by Gran's method,[24] which gives the standard potential, $E^{\circ\prime}$, and the ionic product of water ($pK_w = 13.73(1)$). The concentrations of the different metal ions employed were determined gravimetrically by standard methods.

(7) Bernardo M. A.; Guerrero, J. A.; García-España, E.; Luis, S. V.; Llinares, J. M.; Pina, F.; Ramirez, J. A.; Soriano, C. *J. Chem. Soc., Perkin Trans. 2* **1996**, 2335.
(8) Bernardo, M. A.; Parola, A. J.; Pina, F.; García-España, E.; Marcelino, V.; Luis, S. V.; Miravet, J. F. *J. Chem. Soc., Dalton Trans.* **1995**, 993.
(9) (a) Czarnik, W., Ed. *Fluorescent Chemosensors for Ion and Molecule Recognition;* ACS Symposium Series 538; American Chemical Society: Washington, DC, 1992. (b) *Ibid.*, Chapter 8, p 109. (c) *Ibid.*, Chapter 8, p 113.
(10) Fabbrizzi, L.; Licchelli, M.; Pallavicini, P.; Perotti, A.; Taglietti, A.; Sacchi, D. *Chem. Eur. J.* **1996**, *1*, 75.
(11) Fabbrizzi, L.; Licchelli, M.; Pallavicini, P.; Taglietti, A. *Inorg. Chem.* **1996**, *35*, 1733.
(12) Bissel, R. A.; de Silva, A. P.; Gunaratne, H. Q. N.; Lynch, P. L. M.; Maguire, G. E. M.; Sandanayake, K. R. A. S. *Chem. Soc. Rev.* **1992**, *21*, 187.
(13) Bissel, R. A.; de Silva, A. P.; Gunaratne, H. Q. N.; Lynch, P. L. M.; McCoy, C. P.; Maguire, G. E. M.; Sandanayake, K. R. A. S. *Top. Curr. Chem.* **1993**, *168*, 223.
(14) Huston, M. E.; Haider, K. W.; Czarnik, A. W. *J. Am. Chem. Soc.* **1988**, *110*, 4460.
(15) Sousa, L. R.; Larson, J. M. *J. Am. Chem. Soc.* **1977**, *99*, 307.
(16) Larson, J. M.; Sousa, L. R. *J. Am. Chem. Soc.* **1978**, *100*, 1943.
(17) Shizuka, H.; Takada, K.; Morita, T. *J. Phys. Chem.* **1980**, *84*, 994.
(18) Bouas-Laurent, H.; Castellan, A.; Daney, M.; Desvergne, J.-P.; Guinand, G.; Marsau, P.; Riffaud, M.-H. *J. Am. Chem. Soc.* **1986**, *108*, 315.
(19) Valeur, B.; Bourson, J.; Pouget, J.; Kaschke, M.; Nernsting, N. P. *J. Phys. Chem.* **1992**, *96*, 6545.
(20) Micheloni, M.; May, P.; Williams, D. R. *J. Inorg. Nucl. Chem.* **1978**, *40*, 109.
(21) Micheloni, M.; Sabatini, A.; Vacca, A. *Inorg. Chim. Acta* **1977**, *25*, 41.
(22) García-España, E.; Ballester, M.-J.; Lloret, F.; Moratal, J.-M.; Faus, J.; Bianchi, A. *J. Chem. Soc., Dalton Trans.* **1988**, 101.
(23) Fontanelli, M.; Micheloni, M. *Proceedings of the I Spanish−Italian Congress on Thermodynamics of Metal Complexes;* Diputación de Castellón: Castellón, Spain, 1990.
(24) (a) Gran, G. *Analyst (London)* **1952**, *77*, 881. (b) Rossotti, F. J.; Rossotti, H. *J. Chem. Educ.* **1965**, *42*, 375.

The computer program HYPERQUAD[25] was used to calculate the protonation and stability constants. The titration curves for each system (ca. 100 experimental points corresponding to at least three measurements, pH range investigated 2−10, concentration of metals and **L** ranging from $1 \times 10^{-3}$ to $5 \times 10^{-3}$ mol dm$^{-3}$) were treated either as a single set or as separated curves without significant variations in the values of the stability constants. Finally, the sets of data were merged together and treated simultaneously to give the final stability constants. For the $Ni^{2+}$ systems, a delay of several minutes before each reading was given in order for the systems to reach equilibrium. Moreover, several measurements were made both in formation and in dissociation (from acid to alkaline pH and vice versa) to check the reversibility of the reactions.

**EHMO Calculations**. All calculations were performed by using a package of programs for molecular orbital analysis by Mealli,[26] based on CDNT (atomic Cartesian coordinate calculations), ICON (extended Hückel method with the weighted $H_{ij}$ formula), and FMO (fragment molecular orbital), including the drawing program CACAO (Computer Aided Composition of Atomic Orbitals).

**X-ray Structure Analysis**. Analyses of single crystals of [Cu(**L7**)-$(H_2O)$]$(ClO_4)_2$ were carried out with an Enraf-Nonius CAD-4 single-crystal diffractometer ($\lambda = 0.710\ 73$ Å). The unit cell dimensions were measured from the angular settings of 25 reflections with $\theta$ between 15 and 25°. The space group was $P2_12_12_1$. The reflections were measured in the *hkl* range (0, 0, 0) to (9, 12, 33) between $\theta$ limits of $1 < \theta < 25°$. The $\omega-2\theta$ scan technique and a variable scan rate with a maximum scan time of 60 s per reflection were used. The intensity of the primary beam was checked throughout the data collection by monitoring three standard reflections every 3600 s. The final drift correction factors were in the range 0.98 and 1.02. Profile analysis was performed on all reflections;[27] a semiempirical absorption correction, Ψ-scan based, was performed.[28] In total, there were 2306 "unique" reflections, of which 1350 had $F_o > 4\sigma(F_o)$. Lorenz and polarization corrections were applied, and the data were reduced to $|F_o|$ values. The structure was solved by the Patterson method using the program SHELXS86[29] running on an IBM Pentium 250 computer. Isotropic least-squares refinement was performed with the program SHELXL-93.[30] Hydrogen atoms were placed in calculated positions. Tables 1 and 2 present details of the crystal data and atomic coordinates. Perchlorate counteranions were strongly disordered, in particular, for one of them three of the oxygen atoms of this anion were isotropically refined. Both perchlorate anions were refined with a rigid group restraint.

During the final stages of the refinement the positional parameters and the anisotropic thermal parameters of the non-hydrogen atoms were refined. The hydrogen atoms were refined with a common thermal parameter. The final conventional agreement factors were $R_1 = 0.0572$ and $\omega R_2 = 0.1570$. The maximum shift of the esd ratio in the last full-matrix least-squares cycle was 0.001. The final difference Fourier map showed no peaks higher than 0.86 e Å$^{-3}$ or deeper than −0.63 e Å$^{-3}$. Atomic scattering factors were taken from the *International Tables for X-ray Crystallography*.[31] Molecular plots were produced by the program ORTEP.[32]

(25) Sabatini, A.; Vacca, A.; Gans, P. *Coord. Chem. Rev.* **1992**, *120*, 389.
(26) Mealli, C.; Proserpio, D. *J. Chem. Educ.* **1990**, *67*, 399.
(27) (a) Lehman, M. S.; Larsen, F. K. *Acta Crystallogr., Sect. A* **1974**, *30*, 580. (b) Grant, D. F.; Gabe, E. J. *J. Appl. Crystallogr., Sect A* **1978**, *11*, 114.
(28) Nort, A. C. T.; Philips, Mathews, F. S. *Acta Crystallogr., Sect. A* **1968**, *24*, 351.
(29) Sheldrick, G. M., Kruger, C., Goddard, R., Eds. *Crystallographic Computing*; Clarendon Press: Oxford, 1985; p 175.
(30) Sheldrick, G. M. *SHELXS-93: Program for Crystal Stucture Refinement*; Institute für Anorganische Chemie der Universität Göttingen: Göttingen, Germany, 1993.
(31) *International Tables for X-ray Crystallography*; The Kynoch Press: Birmingham, England, 1974; Vol. IV.
(32) Johnson, C. K. *ORTEP*; Report ORNL-3794; Oak Ridge National Laboratory: Oak Ridge, TN, 1971.

**Table 1.** Crystal Data and Structure Refinement for $[Cu(\mathbf{L7})(H_2O)](ClO_4)_2$

| | |
|---|---|
| compound | $[Cu(\mathbf{L7})(H_2O)](ClO_4)_2$ |
| empirical formula | $C_{15}H_{30}Cl_2CuN_4O_9$ |
| fw | 544.87 |
| cryst color | pink-blue |
| temp | 293(2) K |
| wavelength | 0.710 73 Å |
| cryst syst | orthorhombic |
| space group | $P2_12_12_1$ |
| unit cell dimensions | $a = 7.586(7)$ Å |
| | $b = 10.715(3)$ Å |
| | $c = 28.13(2)$ Å |
| volume | 2286(3) Å$^3$ |
| $Z$ | 4 |
| density (calculated) | 1.583 g cm$^{-3}$ |
| $\mu$ (Mo Kα) | 12.42 cm$^{-1}$ |
| $F$(000) | 1132 |
| cryst size | $0.1 \times 0.2 \times 0.23$ |
| $\theta$ range for data collection | 1−25° |
| index ranges | (0, 0, 0) to (9, 12, 33) |
| no. of reflcns collcd | 2306 |
| no. of indep reflcns | 2306 [$R$(int) = 0.0000] |
| refinement method | full-matrix least-squares on $F^2$ |
| no. of data/restraints/params | 2288/2/263 |
| goodness-of-fit on $F^2$ | 1.021 |
| final $R$ indices [$I > 2\sigma(I)$] | $R_1 = 0.0572$, $wR_2 = 0.1570$ |
| $R$ indices (all data) | $R_1 = 0.1341$, $wR_2 = 0.1821$ |
| largest diff. peak and hole | 0.860 and −0.627 e Å$^{-3}$ |

[a] $R_1 = \Sigma||F_o| - |F_c||/\Sigma|F_o|$. [b] $wR_2 = [\Sigma w(F_o^2 - F_c^2)^2/\Sigma w(F_o^2)^2]$, $w = 1/[\sigma^2(F_o)^2 + (0.1056P)^2]$; $P = [(\max(F_o^2) + 2(F_c)^2])$.

**Table 2.** Atomic Coordinates ($\times 10^4$) and Equivalent Isotropic Displacement Parameters (Å$^2 \times 10^3$) for **1**[a]

| | *x/a* | *y/b* | *z/c* | *U*(eq)[b] |
|---|---|---|---|---|
| Cu(1) | 8503(2) | 2195(1) | 8765(1) | 34(1) |
| Cl(1) | 2620(4) | 2957(3) | 9462(1) | 39(1) |
| O(11) | 1393(14) | 2035(9) | 9351(3) | 75(3) |
| O(12) | 4141(12) | 2435(10) | 9678(3) | 71(3) |
| O(13) | 3133(13) | 3577(11) | 9025(3) | 82(3) |
| O(14) | 1806(17) | 3838(10) | 9770(3) | 87(4) |
| Cl(2) | 4164(5) | 5310(4) | 7661(1) | 71(1) |
| O(21) | 3893(14) | 4758(8) | 8114(2) | 85(3) |
| O(22) | 3594(18) | 4445(8) | 7352(2) | 162(6) |
| O(23) | 2895(15) | 6312(9) | 7665(4) | 204(8) |
| O(24) | 5655(11) | 6037(11) | 7640(4) | 214(9) |
| O$1(1) | −4044(12) | 2568(7) | 8270(3) | 55(2) |
| N(1) | 7434(16) | 639(9) | 9095(4) | 40(3) |
| N(2) | 9672(14) | 1111(10) | 8276(3) | 43(3) |
| N(3) | 9759(15) | 3629(11) | 8417(4) | 53(3) |
| N(4) | 7643(14) | 3317(9) | 9290(3) | 45(3) |
| C(1) | 5814(17) | 219(10) | 8872(4) | 43(3) |
| C(2) | 8801(19) | −412(13) | 9162(6) | 64(4) |
| C(3) | 9510(21) | −866(13) | 8709(7) | 75(5) |
| C(4) | 10655(19) | 23(14) | 8451(5) | 66(4) |
| C(5) | 10817(18) | 1877(14) | 7974(4) | 64(4) |
| C(6) | 10066(20) | 3184(15) | 7941(4) | 67(5) |
| C(7) | 8607(26) | 5353(13) | 8925(6) | 75(5) |
| C(8) | 8971(23) | 4884(11) | 8444(5) | 66(4) |
| C(9) | 7280(22) | 4621(12) | 9198(5) | 61(4) |
| C(11) | 4897(17) | −902(10) | 9089(4) | 41(3) |
| C(12) | 4560(17) | −1949(10) | 8833(4) | 48(3) |
| C(13) | 3774(18) | −2965(12) | 9015(5) | 56(3) |
| C(14) | 3180(19) | −2946(11) | 9488(5) | 58(4) |
| C(15) | 3557(24) | −1996(14) | 9760(5) | 78(5) |
| C(16) | 4298(24) | −881(13) | 9556(4) | 68(4) |

[a] Symmetry operations for equivalent atoms: \$1, $x - 1$, $y$, $z$; \$2, $x + 1$, $y$, $z$. [b] $U$(eq) is defined as one-third of the trace of the orthogonalized $\mathbf{U}_{ij}$ tensor.

## Results and Discussion

**Potentiometric Studies.** In Tables 3−5 we report the stability constants of the $Co^{2+}$, $Ni^{2+}$, $Cu^{2+}$, $Zn^{2+}$, $Cd^{2+}$, and

**Table 3.** Logarithms of the Stability Constants for the $Co^{2+}$ or $Ni^{2+}$ Complexes of Ligands **L1**−**L4** Determined by Potentiometry at 298.0 ± 0.1 K in 0.15 mol $dm^{-3}$ $NaClO_4$ or 0.15 mol $dm^{-3}$ NaCl[a]

| | **L1**[c] | | **L2**[c] | | **L3**[c] | | **L4**[a] | |
|---|---|---|---|---|---|---|---|---|
| reaction[b] | $Co^{2+}$ | $Ni^{2+}$ | $Co^{2+}$ | $Ni^{2+}$ | $Co^{2+}$ | $Ni^{2+}$ | $Co^{2+}$ | $Ni^{2+}$ |
| M + L = ML | 6.03(3)[c] | 8.32(2) | 9.33(1) | 12.17(2) | 12.67(2) | 15.48(6) | 6.09(2) | 10.14(2) |
| MHL + H = $MH_2L$ | | | | | 5.96(6) | | | |
| ML + H = MHL | | | 6.03(5) | 4.8(1) | 6.19(5) | 4.9(1) | 8.71(4) | 6.6(2) |
| ML + OH = ML(OH) | 4.76(6) | 4.43(7) | 3.99(4) | 3.99(7) | 3.75(7) | | 3.34(5) | |

[a] 0.15 mol $dm^{-3}$ NaCl. [b] Charges omitted for clarity. [c] Values in parentheses are standard deviations in the last significant figure.

**Table 4.** Logarithms of the Stability Constants for the $Cu^{2+}$ and $Zn^{2+}$ Complexes of Dibenzylated Polyamines **L1**−**L4** and of Cyclophanes **L5**−**L6** Determined by Potentiometry (pot) and/or by emission Fluorescence (fluor) at 298.0 ± 0.1 K in 0.15 mol $dm^{-3}$ $NaClO_4$ or 0.15 mol $dm^{-3}$ NaCl[a]

| | **L1** | | **L2** | | **L3** | | **L4**[a] | | **L5** | | **L6** | |
|---|---|---|---|---|---|---|---|---|---|---|---|---|
| reaction[b] | pot | fluor | pot | fluor | pot | fluor | pot | fluor | pot | fluor | pot | fluor |
| Cu + L = CuL | 13.91(1)[c] | 15.3(2) | 19.50(2) | 20(1) | 21.06(5) | 21.2(2) | 17.30(2) | 17.3(2) | 10.41(2)[d] | | 13.02(1)[d] | |
| CuL + H = CuHL | 3.33(4) | 3.3(3) | 3.12(5) | 3.1(4) | 4.96(8) | 5.5(5) | 5.45(3) | 5.4(2) | 6.51(3)[d] | | 7.80(1)[d] | |
| CuHL + H = $CuH_2L$ | | | | | 3.71(8) | 3.7(5) | | | | | | |
| CuL + OH = CuL(OH) | 5.08(3) | *e* | 4.37(8) | *e* | | | | | 5.59(7)[d] | | 4.63(1)[d] | |
| Zn + L = ZnL | 6.60(1) | 8.0(4) | 10.47(1) | 10.8(5) | 13.63(2) | 14.1(4) | 7.68(1) | 7.7(2) | 4.55(4) | *e* | 6.83(1)[d] | *e* |
| ZnL + H = ZnHL | | | | | 5.50(6) | 5.0(3) | 7.86(2) | 7.9(2) | | | 7.77(2)[d] | 7.8(2) |
| ZnL + OH = ZnL(OH) | 4.88(4) | 5.0(1) | 5.61(5) | 5.6(2) | 2.81(9) | 2.81(9) | 4.26(2) | 4.3(2) | 5.48(5) | *e* | 5.05(3)[d] | 5.1(4) |
| ZnL(OH) + OH = $ZnL(OH)_2$ | 3.42(9) | 3.4(2) | 3.97(8) | 4.3(2) | | | | | 3.63(8) | *e* | | |

[a] 0.15 mol $dm^{-3}$ NaCl. [b] Charges omitted by clarity. [c] Values in parentheses are standard deviations in the last significant figure. [d] Values taken from refs 1−3. [e] Spectrofluorimetry is not sensitive enough to evaluate these constants.

**Table 5.** Logarithms of the Stability Constants for the Formation of $Cd^{2+}$ and $Pb^{2+}$ Complexes of the Ligands **L1**−**L4** determined by Potentiometry at 298.1 ± 0.1 K in 0.15 mol $dm^{-3}$ $NaClO_4$ or in 0.15 mol $dm^{-3}$ NaCl[a]

| | **L1** | | **L2** | | **L3** | | **L4**[a] |
|---|---|---|---|---|---|---|---|
| reaction[b] | $Cd^{2+}$ | $Pb^{2+}$ | $Cd^{2+}$ | $Pb^{2+}$ | $Cd^{2+}$ | $Pb^{2+}$ | $Cd^{2+}$ |
| M + L = ML | 6.31(1)[b] | 6.81(1) | 9.75(2) | 9.68(2) | 12.44(2) | 10.61(2) | 7.16(1) |
| ML + H = MHL | | | 5.6(1) | | 5.76(4) | 6.93(4) | 8.27(2) |
| ML + OH = ML(OH) | 3.84(6) | 5.00(3) | 3.70(6) | 3.84(5) | 3.17(8) | 3.68(6) | 2.73(2) |

[a] 0.15 mol $dm^{-3}$ NaCl. [b] Charges have been omitted for clarity. [c] Numbers in parentheses are standard deviations in the last significant figure.

$Pb^{2+}$ complexes of ligands **L1**−**L4**. The formation constants of $Cu^{2+}$ and $Zn^{2+}$ complexes of *p*-azacyclophanes **L5** and **L6** (see Chart 1) are included in Table 4. All the constants have been determined at 298.1 ± 0.1 K in 0.15 mol $dm^{-3}$ $NaClO_4$, but those of **L4** that were determined in 0.15 mol $dm^{-3}$ NaCl due to the low solubility in the former medium of the complexes of this ligands.

An analysis of the different systems reveals several aspects. First of all, in all the systems only species of 1:1 stoichiometry, either neutral or hydroxylated, have been detected even when a large excess of ligand was used in the potentiometric measurements. The steric hindrance imposed by the benzylic moieties, preventing the approach of a second ligand, should explain this behavior.

Concerning stability, the first aspect to be remarked is that the stability constants of the $[ML]^{2+}$ species essentially follow, in all the systems, the general Irving−Williams order of stability.

Also of interest are the lower magnitudes of the formation constants of the benzylated ligands in comparison with those of the related open-chain nonbenzylated polyamines **L8**−**L10**. For instance, decreases ranging from 1 to 2 logarithmic units are observed between the $[ML]^{2+}$ complexes of $Co^{2+}$, $Ni^{2+}$, $Cu^{2+}$, $Cd^{2+}$, and $Pb^{2+}$ of **L2** and those of diethylenetriamine (**L8**).[33] This general behavior can be extended to all the terms of the series, with the only exception of complex $[Pb\mathbf{L3}]^{2+}$ (Table 5), which presents a stability comparable to that of complex $[Pb\mathbf{L10}]^{2+}$ (log $K$ = 10.2).[33] However, when the stability constants for both series of complexes, benzylated and nonbenzylated, are plotted versus the overall basicity of the ligands (log $\beta = \Sigma \log K_{HiL}$), a linear tendency is obtained in all cases. As an example, in Figure 1 is represented the plot for the $Cu^{2+}$, $Ni^{2+}$, and $Co^{2+}$ complexes. This yields scarce selectivity of one type of ligand over the other in the binding of a determined metal ion.

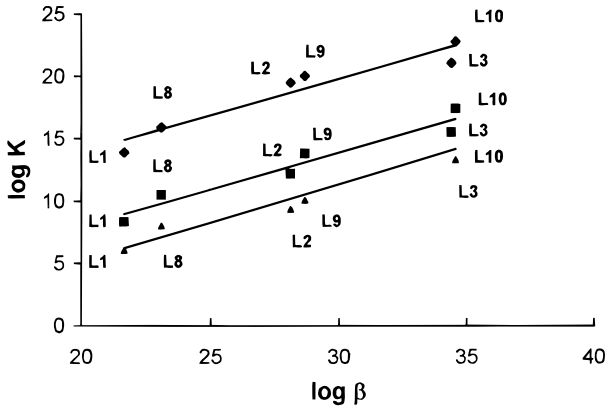


**Figure 1.** Representation of the stability constants of the $[CuL]^{2+}$ (◆), $[NiL]^{2+}$ (■), and $[CoL]^{2+}$ (▲) complexes of ligands **L1**−**L3**, **L8**−**L10** as a function of the overall basicity of the ligands (log $\beta = \Sigma \log K_{HiL}$).

On the other hand, the formation constants for the $Cu^{2+}$ or $Zn^{2+}$ complexes of **L2** and **L4** are clearly higher than those of

(33) Martell, A. E.; Smith, R. M.; Moteikaitis, R. M. *NIST Critical Stability Constants Database*; Texas A&M University: College Station, TX, 1993.

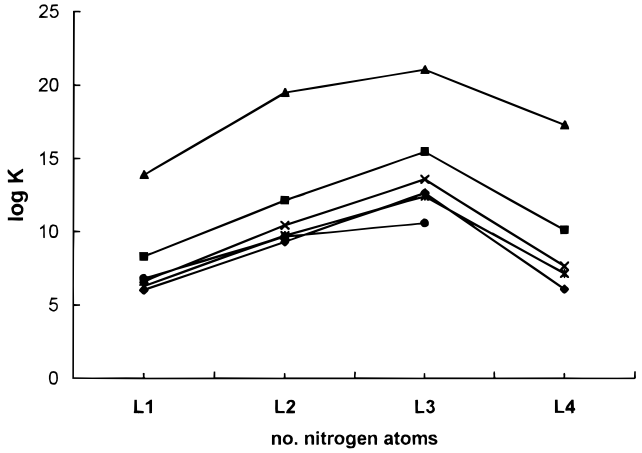


**Figure 2.** Plot of the formation constants of the $[ML]^{2+}$ species for the complexes formed between the bivalent metal ions $Co^{2+}$ (◆), $Ni^{2+}$ (■), $Cu^{2+}$ (▲), $Zn^{2+}$ (×), $Cd^{2+}$ (*), and $Pb^{2+}$ (●) with ligands **L1**−**L4**.

the related complexes of the *p*-azacyclophane ligands **L5** and **L6** (Table 4).[1,3] This would further confirm the role played by the phenylene spacer in these macrocycles in preventing the simultaneous coordination of both benzylic nitrogens to the same metal center.

Although it is difficult to establish the number of bound nitrogens from just the free energy terms, in some favorable cases, the magnitude of the stability constants, the number of protonated species formed as well as the tendencies of the stability values may provide light in this respect.

In Figure 2 are plotted the stability constants for the formation of ML complexes by ligands **L1**−**L4**. Inspection of this figure shows that for $Co^{2+}$, $Ni^{2+}$, $Zn^{2+}$, and $Cd^{2+}$ the stability constants steadily increase along the series. These data suggest that, for these metal ions, an increasing number of nitrogen donors are involved in the coordination to the different metals along the series. For $Cu^{2+}$ and $Pb^{2+}$ a steady increment is produced on going from **L1** to **L2**, the stability of the $[ML2]^{2+}$ and $[ML3]^{2+}$ complexes being very close, however. So in these last cases, the data suggest that the fifth nitrogen in **L3** would be either noncoordinated or less tightly coordinated than the first four nitrogen atoms. Indeed, this is not so surprising in the chemistry of $Cu^{2+}$ due to the Jahn−Teller axial distortion that this metal ion usually exhibits. The crystal structure of the monobenzylated ligand **L7** is reflecting such a situation. In this complex it can be seen that $Cu^{2+}$ is coordinated in a very distorted square-pyramidal fashion by the four nitrogen atoms disposed at the vertexes of the square (Cu−N(1), 2.073(10) Å; Cu−N(2), 2.006(9) Å; Cu−N(3), 2.056(11) Å; Cu−N(4), 2.013(9) Å) occupying a water molecule the axial position with a very long Cu−O distance of 2.415(9) Å.

**Absorption and Fluorescence Emission Studies. Zinc Complexes.** For both families of compounds reported in Chart 1, we observed that the UV−visible absorption spectra obtained in the presence and in the absence of $Zn^{2+}$ does not change substantially, as reported by Czarnik for the interaction of this metal ion with several anthrylazamacrocycles.[9b] The lack of new absorption bands, upon coordination to the metal, indicates that the excited state of the adduct remains ligand centered.

Concerning the titration curves obtained by steady-state fluorescence emission in which no experimental evidences for the formation of excimers were found, the two families present distinct behavior. For the polyazacyclophane ligands, the presence of $Zn^{2+}$ leads to a small CHEF effect for the ligand **L6**, and no effect for **L5.** In contrast, for the N,N′-dibenzylated

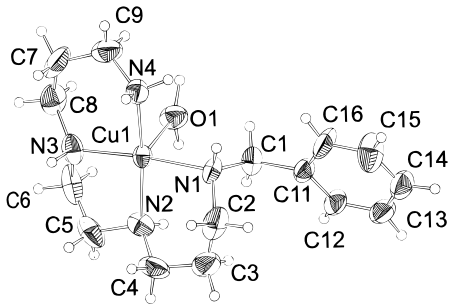


**Figure 3.** ORTEP drawing of the $[CuL7(H_2O)]^{2+}$ cation. Thermal ellipsoids are drawn at the 30% probability level.

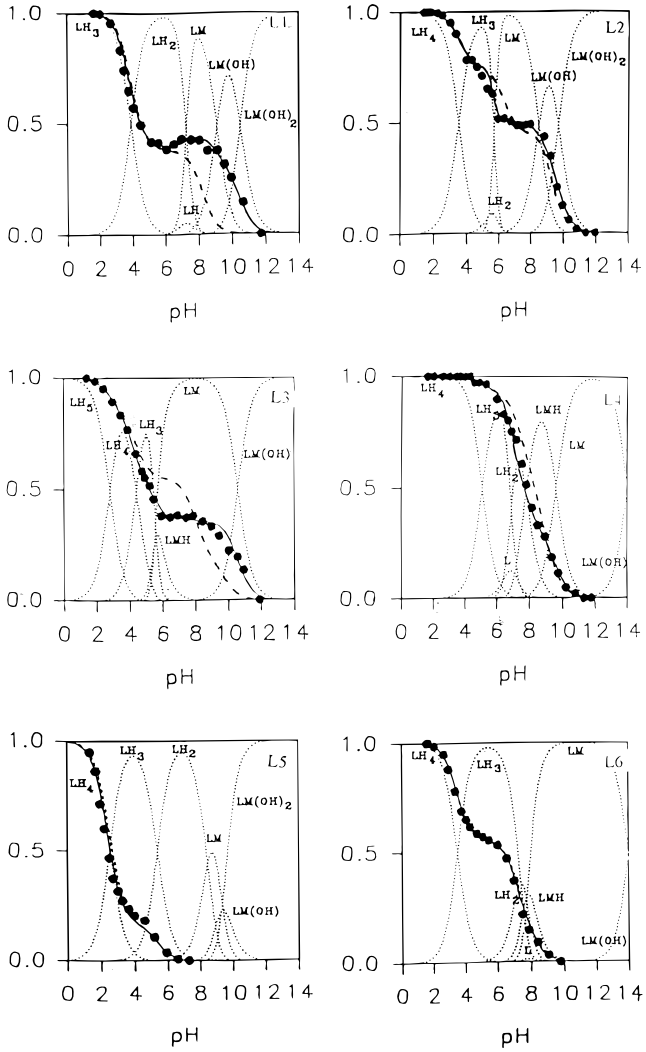


**Figure 4.** Steady-state fluorescence emission titration curves of polyamines **L1**−**L6**, at the excitation and emission wavelengths, respectively 264 and 290 nm, in the presence and absence of equimolar amounts of $Zn^{2+}$ (solid and traced lines, respectively). Molar fraction distributions in the presence of $Zn^{2+}$ are also represented by the dotted line.

open-chain polyamines significant CHEF and CHEQ effects can be detected in the presence of $Zn^{2+}$ as reported in Figure 4.

The fitting to the experimental values was carried out using the approach described elsewhere,[7,8] taking the protonation and stability constants measured by potentiometry as an initial guess. In general, a good agreement between the constants calculated by potentiometry and those obtained by spectrofluorimetry was observed (see Table 4). From the fitting we can obtain the ratios between the fluorescence emission quantum yields of the fully

**Table 6.** Ratios between the Fluorescence Emission Quantumn Yields of $Zn^{2+}$ Complexes and the Respective Fully Protonated Form of the Free Ligand[a]

| | L1 | L2 | L3 | L4 | L5 | L6 |
|---|---|---|---|---|---|---|
| ZnHL[b] | | | 0.70 | 0.50 | | 0.40 |
| ZnL | 0.45 | 0.55 | 0.25 | 0.40 | *c* | *c* |
| ZnL(OH) | 0.35 | 0.48 | *c* | *c* | *c* | *c* |

[a] Estimated error 5%. [b] Charges omitted for clarity. [c] No emission.

protonated species of the free ligands and those of the different emissive metal complexes. Inspection of Table 6 shows that all the emissive complexes present fluorescence quantum yields lower than the respective quantum yields of the fully protonated forms of the free ligands. In the case of the ligands **L1** and **L2**, three complexes, $[ZnL]^{2+}$, $[ZnL(OH)]^{+}$, and $[ZnL(OH)_2]$ are detected by potentiometry. We observed emission from $[ZnL]^{2+}$ and $[ZnL(OH)]^{+}$ but not from $[ZnL(OH)_2]$. For the latter complexes partial decomplexation at this stage could explain this behavior. In all these complexes the nitrogens would be fully involved in the coordination to the metal. The $Zn^{2+}$ complexes display an emission with quantum yield ca. half of the emission detected for the fully protonated forms of the free ligands. This implies that coordination with $Zn^{2+}$, similarly to protonation, prevents the PET between the amines and the fluorophore, but with less efficiency. When the water coordinated to the $Zn^{2+}$ loses a proton, the protective effect of the $Zn^{2+}$ cation decreases and ceases completely by removal of a second proton from another water ligand. Concerning the two remaining ligands of this family, **L3** and **L4**, the potentiometric titrations predict the existence of the species $[ZnHL]^{3+}$, $[ZnL]^{2+}$, and $[ZnL(OH)]^{+}$. These results are also consistent with the data obtained from the fluorescence emission titration curves. In effect, in both cases emission from $[ZnHL]^{3+}$ and $[ZnL]^{2+}$ is observed. In these complexes, all the lone pairs of the nitrogen donors are protected from PET either by the metal ion or by the proton. In $[ZnH\mathbf{L4}]^{3+}$ three nitrogen lone pairs would be shared with the metal ion and one with the proton, while in the $[ZnH\mathbf{L3}]^{3+}$ complex of the pentaamine **L3**, four with the metal and one with the proton would be shared. Finally the $[ZnL]^{2+}$ species are also emissive because, as in the previous cases, all the nitrogens are protected from PET, now exclusively by coordination to $Zn^{2+}$. By comparing the relative intensities of the fluorescence emissions of the $[ZnHL]^{3+}$ and $[ZnL]^{2+}$ complexes (Table 6) it can be seen that the former are higher. This result is again in agreement with the more efficient CHEF effect of protonation than of $Zn^{2+}$ coordination, in accordance with previous work reported for other systems.[9b]

The complexes of macrocycles **L5** and **L6** show important differences in comparison with the N,N′-dibenzylated open-chain polyamines containing four nitrogens (**L2** and **L4**). These macrocycles coordinate metal ions through a maximum of three of their four nitrogen donors due to the relatively high rigidity of this type of ligands.[1,3−6,8] According to the potentiometric studies, three metal complexes $[ZnL]^{2+}$, $[ZnL(OH)]^{+}$, and $[ZnL(OH)_2]$, are expected for **L5**. In all these complexes, one of the benzylic nitrogens is neither protonated nor coordinated, and thus can be involved in a PET quenching effect, explaining the absence of the emission. The coincidence of the fluorescence emission titration curves in the presence and absence of $Zn^{2+}$ can be explained as follows: (i) in the free ligand only $H_4L^{4+}$ and $H_3L^{3+}$ are emissive; (ii) since the association constants are low, the molar fraction distributions as a function of pH of the emissive species $H_4L^{4+}$ and $H_3L^{3+}$ are not significantly affected by coordination to the metal.

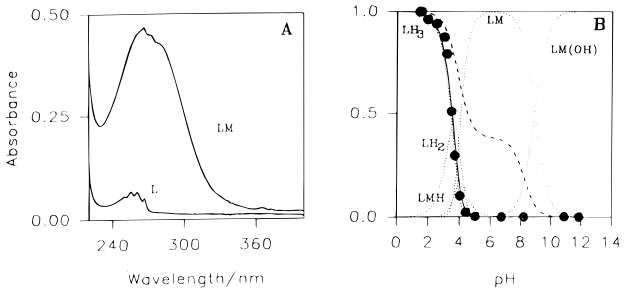


**Figure 5.** Ligand **L1**, $10^{-4}$ M, in the presence of equimolar amounts of $Cu^{2+}$. (A) Absorption spectrum at pH = 6; (B) fluorescence emission titration curve (solid line); we represent also the titration curve of the free ligand for comparison purposes (traced line). Molar fraction distributions in the presence of $Cu^{2+}$ are also depicted (dotted line).

**Scheme 1**

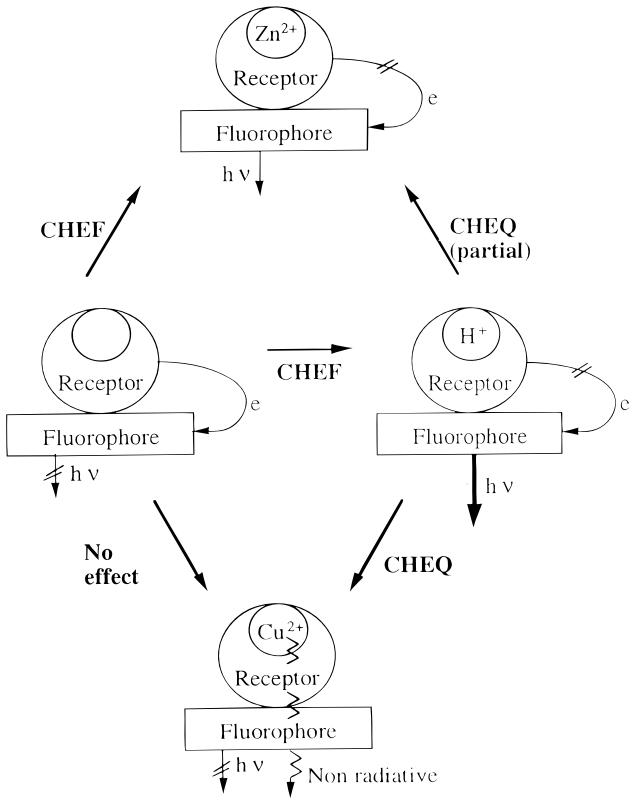


For the *p*-azacyclophane **L6** the complex species predicted by potentiometry are $[ZnHL]^{3+}$, $[ZnL]^{2+}$, and $[ZnL(OH)]^{+}$.[1] In this case, only the $[ZnHL]^{3+}$ species presents all its nitrogen donors either coordinated to $Zn^{2+}$ (three nitrogens) or protonated (one nitrogen), preventing the PET effect and allowing fluorescence emission to be observed (Table 6). The practical absence of net effects on the titration curves in the presence and absence of $Zn^{2+}$ is now due to the following reasons: (i) in the free ligand, $H_4L^{4+}$ and $H_3L^{3+}$ are again the only emissive species; (ii) the association constant of $[ZnHL]^{3+}$ is higher than in the previous example of **L5**, and by consequence the molar fraction distribution of $H_3L^{3+}$ slightly decreases; (iii) however, this effect is counterbalanced through the formation of the emissive complex $[ZnHL]^{3+}$.

In general $Zn^{2+}$ complexation gives rise to two different effects (see Figure 4 and Scheme 1): (i) the molar fraction distributions of the highly protonated and emissive forms of the free ligand are decreased and shifted to lower pH values and the ligands are substituted by less emissive metal complexes, explaining the CHEQ effect, and (ii) the existence of emissive

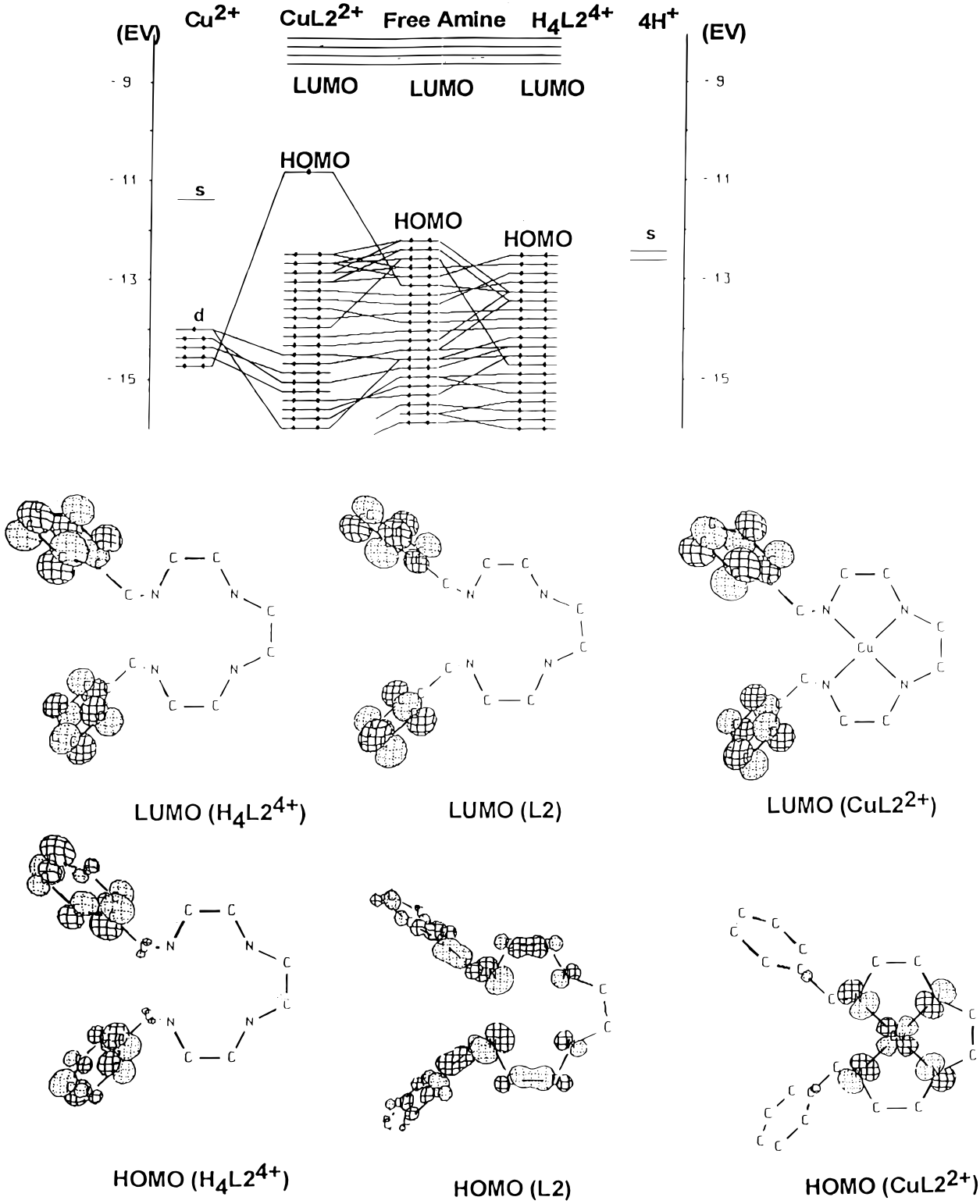


**Figure 6.** Frontier molecular orbitals for **L2**, $H_4$**L2**$^{4+}$, and [Cu**L2**]$^{2+}$.

metal complexes is allowed at moderately basic pH regions where, in the absence of metal, no emissive species of the free ligand are present, leading to a CHEF effect. These two effects are thus the result of the existence of differentiated domains for each kind of emissive species.

CHEF effects were also observed in the interaction of $Cd^{2+}$ with these ligands, but the protective effect of this metal ion is lower than that of $Zn^{2+}$. For example, the ratios of the quantum yields between the complexes [CdH**L3**]$^{3+}$ and [Cd**L3**]$^{2+}$ and the fully protonated receptor $H_5$**L3**$^{5+}$ (0.22 and 0.10, respectively), are less than one-half of those found for the corresponding $Zn^{2+}$ complexes.

In conclusion, the CHEF effect follows the order $H^+ > Zn^{2+} > Cd^{2+}$. This behavior could be related to the ability of these ions to remove electron density from the nitrogen, which is proportional to their charge density.[9c] Although PET is proposed as the major pathway for the nonradiative deactivation, other possible routes based on the influence of the metals on the nonradiative deactivation process, like the heavy-atom effect in cadmium complexes, could also be operative.

**Copper Complexes.** In contrast with the $Zn^{2+}$ complexes, the $Cu^{2+}$ complexes of both families of ligands promote large increases on the molar absorption coefficients as well as blue shifts on the UV-visible absorption maxima. These new and very intense absorption bands (see Figure 5A) are characteristic of charge-transfer processes[34] and denote large interactions between the molecular orbitals of the ligand and those of the metal. As a consequence, the excited states are no longer centered in the ligand but display metal character.

Concerning fluorescence, no emission was observed for these complexes and the recorded fluorescence spectra are due only to the protonated forms of the free ligands[35] (Figure 5B). Again, in this case, no experimental evidence for the formation of excimers was found.

According to the potentiometric studies several species with all the nitrogens involved in the coordination to the metal ion and/or in protonation are present in solution. Despite this, no emission was observed. A possible explanation for the absence of fluorescence emission in the copper complexes can be found on the charge-transfer characteristic of the excited state, which can provide a channel through the metal for the deactivation of the excited state (see Scheme 1). A similar explanation was reported by Fabbrizzi et al.[10,11] In their case the fluorophore is the anthracene moiety and the receptor is a quadridentate aza crown or its open-chain counterpart. According to these authors $Cu^{2+}$ is able to transfer an electron to the excited fluorophore. In our receptors the charge-transfer band observed in the absorption spectra can further support such a mechanism.

Finally we observed that $Pb^{2+}$ complexes of both families behave like $Cu^{2+}$. Similar reasons can be argued due to the detection also in these adducts of a charge-transfer band.

**Molecular Orbital Calculations**. Initial molecular orbital calculations have been performed on the nonprotonated and fully protonated forms of **L2** as well as on its $[Cu\mathbf{L2}]^{2+}$ and $[Zn\mathbf{L2}]^{2+}$ complexes. Such a treatment reveals that while the LUMO orbitals are, in all cases, formed exclusively by the atomic orbitals of the benzene moiety, the composition and energy of the HOMO orbitals are strongly affected either by the protonation degree of the polyamines or by the coordination to metal ions (Figure 6). Indeed, while the HOMO of $H_4\mathbf{L2}^{4+}$ is essentially made up by the atomic orbitals of the aromatic rings, an important contribution to the HOMO of the orbitals of the nitrogen and carbon atoms of the aliphatic portion is observed in the nonprotonated form. Although changes in the conformation of the ligand affect the energy of the frontier orbitals, they do not seem to significantly affect its composition. For instance, a change of the $H_4\mathbf{L2}^{4+}$ conformation to a more elongated one shows a similar composition of the frontier orbitals. This would explain the absence of emission of the nonprotonated forms of this polyamines. The calculations for $[Cu\mathbf{L2}]^{2+}$, for which square-planar coordination geometry has been assumed, show that while the LUMO is again the same, the HOMO is made up by atomic orbitals of the nitrogen atoms and d orbitals of the metal ion. Although the d atomic orbitals contribute to the HOMO change, similar conclusions can be drawn when other coordination geometries are considered. Also, molecular orbitals calculations based on the crystallographic data of $[Cu(\mathbf{L7})(H_2O)](ClO_4)$ yield similar results with respect to the composition of the frontier orbitals.

Similar treatment for $[Zn\mathbf{L2}]^{2+}$ shows that, also in this case, the LUMO remains unaffected by the coordination of $Zn^{2+}$ and that, unlike $Cu^{2+}$ and independently of the coordination geometry, there is no participation of the metal ion atomic orbitals in the HOMO. This orbital remains ligand-centered, presenting an important contribution of the aromatic orbitals in agreement with the observed CHEF effects.

**Conclusion.** Comparison of the properties of these two fluorescent chemosensor families of compounds shows that N,N′,-dibenzylated open-chain polyamines are more appealing than polyazacyclophanes. In the case of $Cu^{2+}$, N,N′-dibenzylated open-chain polyamines only present a CHEQ effect, but with $Zn^{2+}$ these ligands are more versatile presenting opposite effects (CHEQ and CHEF) depending on the pH domain. According to the diagrammatic representation introduced by De Silva et al.,[12,13] our chemosensors can be accounted for by Scheme 1.

Actually we are extending these studies to other transition and post-transition metal ions as well as designing new sensors with even larger signaling efficiency and selectivity.

**Acknowledgment.** We are indebted to DGICYT Project No. PB96-0792 and Portuguese Junta Nacional de Investigação Cientifica e Tecnologica (Praxis XXI/BD/4504/94) for financial support.

**Supporting Information Available:** Tables of bond lengths and angles (Table S1), torsion angles (Table S2), and anisotropic displacement parameters (Table S3) and a figure with EHMO calculations for $H_4\mathbf{L2}^{4+}$ in elongated conformation are available (6 pages). Ordering information is given on any current masthead page.

IC970840N

(34) Horvath, O.; Stevenson, K. L. *Charge-transfer photochemistry of coordination compounds*; VCH: Weinheim, Germany, 1993.

(35) In this case the fluorescence method can only account for the shifts on the molar fraction distribution of the highly protonated species $LH_n^{n+}$ and $LH_{n-1}^{(n-1)+}$. These species are largely affected due to high association contants with $Cu^{2+}$.